Instruments and methods for biomedical applications

Vladimir Solovov

Jornadas do LIP
Pavilhão do Conhecimento, April 27, 2015

The projects

PET with Resistive Plate Chambers (RPC-PET)

- Paulo Fonte
- Alberto Blanco
- Americo Pereira
- Carlos Silva
- Joaquim Oliveira
- Miguel Couceiro
- Nuno Carolino
- Orlando Cunha
- Paulo Crespo
- Ricardo Caeiro
- Rui Alves
- Rui Marques

Detectors and Monte Carlo in Medical Physics

- Luis Peralta
- Alina Louro
- Ana Campos
- Conceicao Abreu
- Florbela Rego
- Joao Antunes
- Jorge Sampaio
- Patrick Sousa
- Pedro Gabriel Almeida
- Rui Carvalhal
- Sandra Soares

The projects

Orthogonal Ray Imaging for Radiotherapy Improvement (OrthoCT)

- Paulo Crespo
- Hugo Simoes
- Patricia Cambraia Lopes
- Sonia Sousa

Adaptive methods for medical imaging with gamma cameras (GAMMA)

- Vladimir Solovov
- Andrei Morozov
- Francisco Fraga
- Francisco Neves
- Joao Marcos
- Luis Pereira
- Raimundo Martins
- Valdemar Domingos
- Vitaly Chepel

Wide Axial Field-of-View (AFOV) PET

[D.B.Crosetto, 2000]

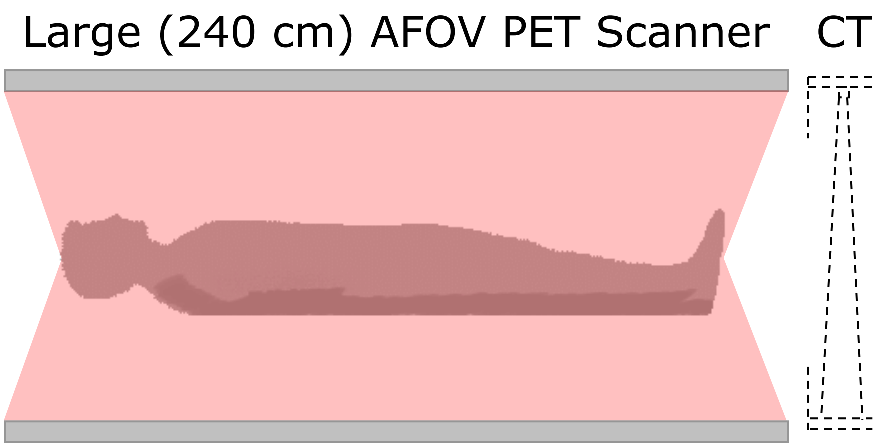

Advantages compared to standard limited AFOW PET:

- High geometric efficiency
- Whole body image obtained in one go
- Continuous uptake signal
- Lower injected activity
- Lower cost per exam

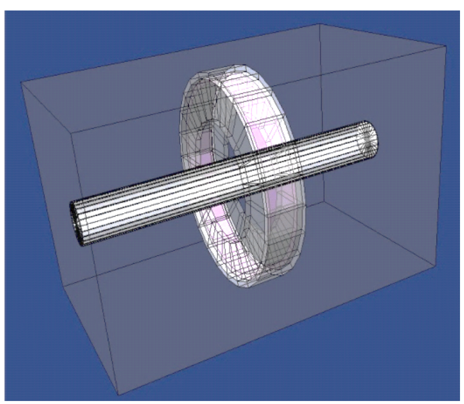

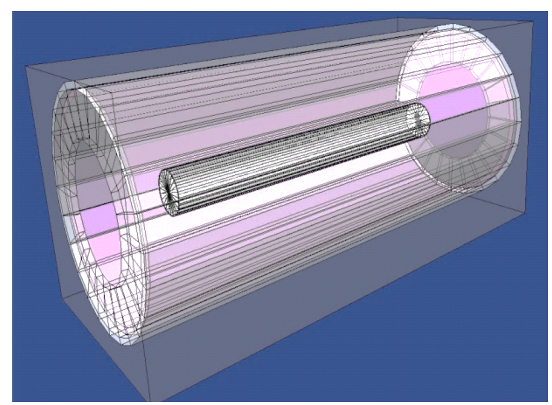

[M.Couceiro et al.,

RPC TOF-PET Geometry

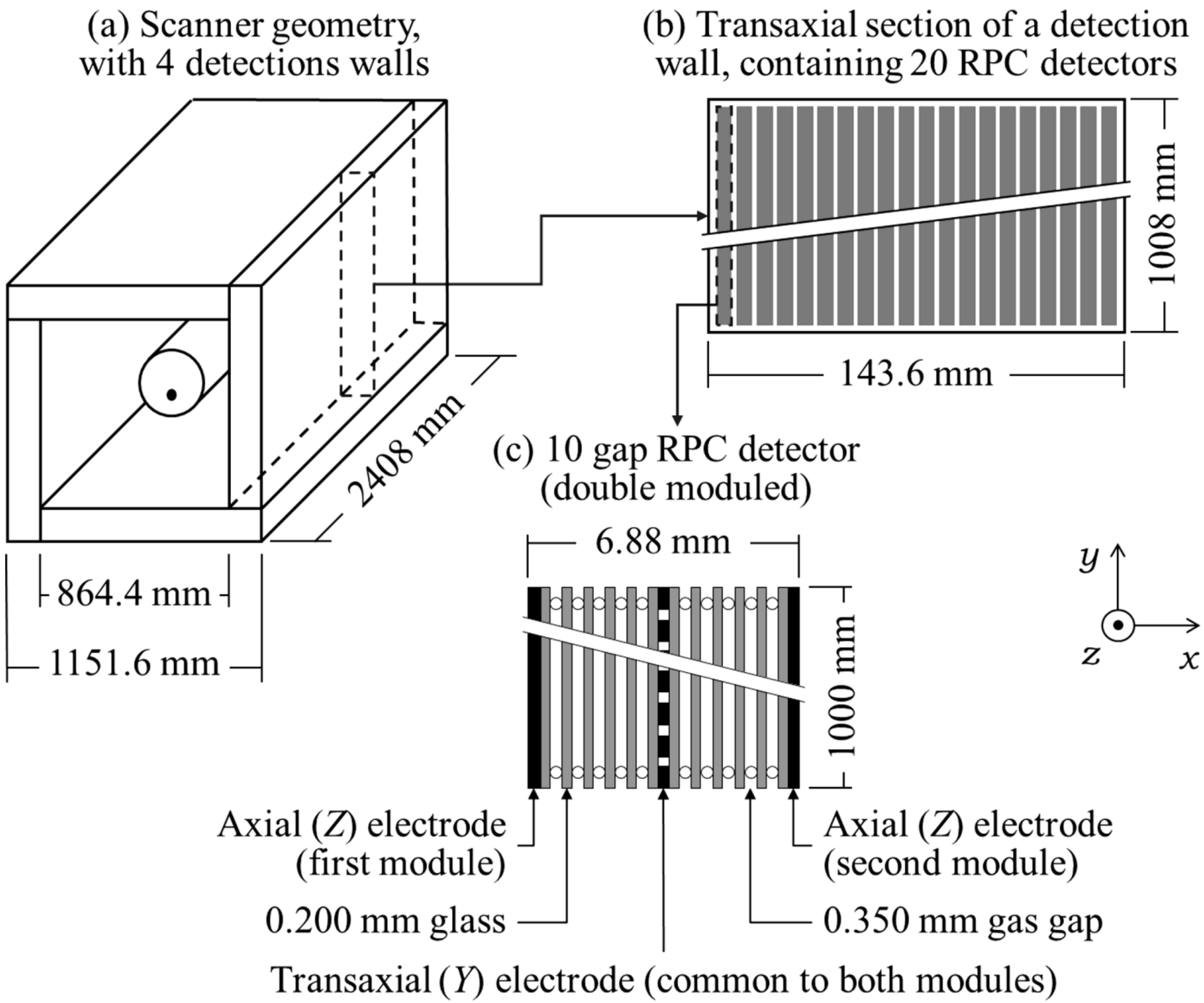

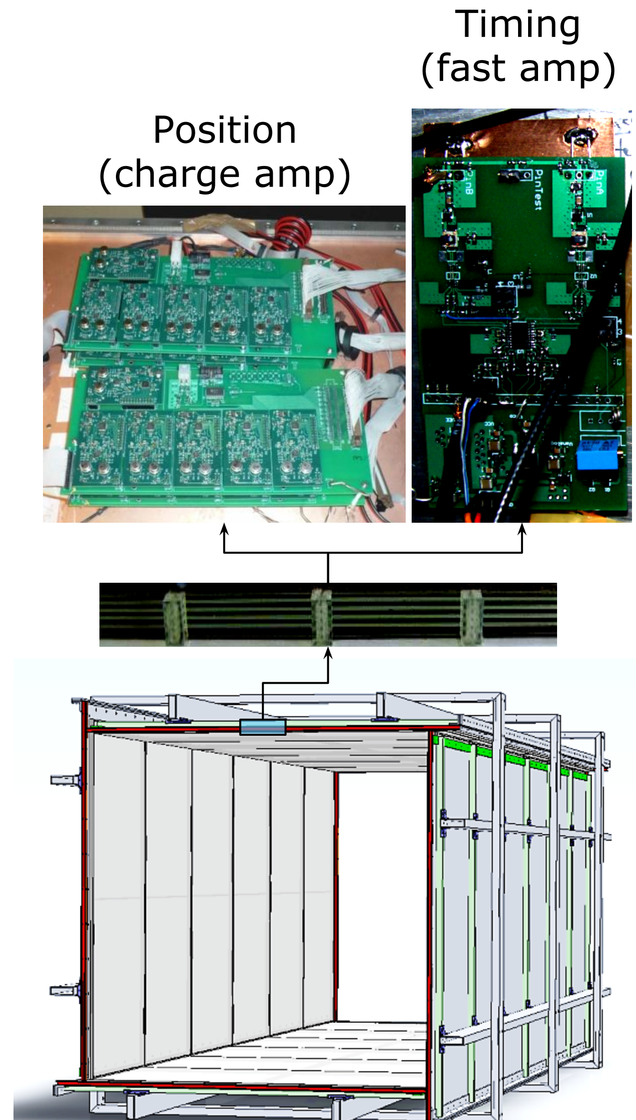

RPC TOF-PET: simulations

Noise Equivalent count Rate (NECR)

- NECR and NECR gain relative to that of the Philips Gemini TF scanner

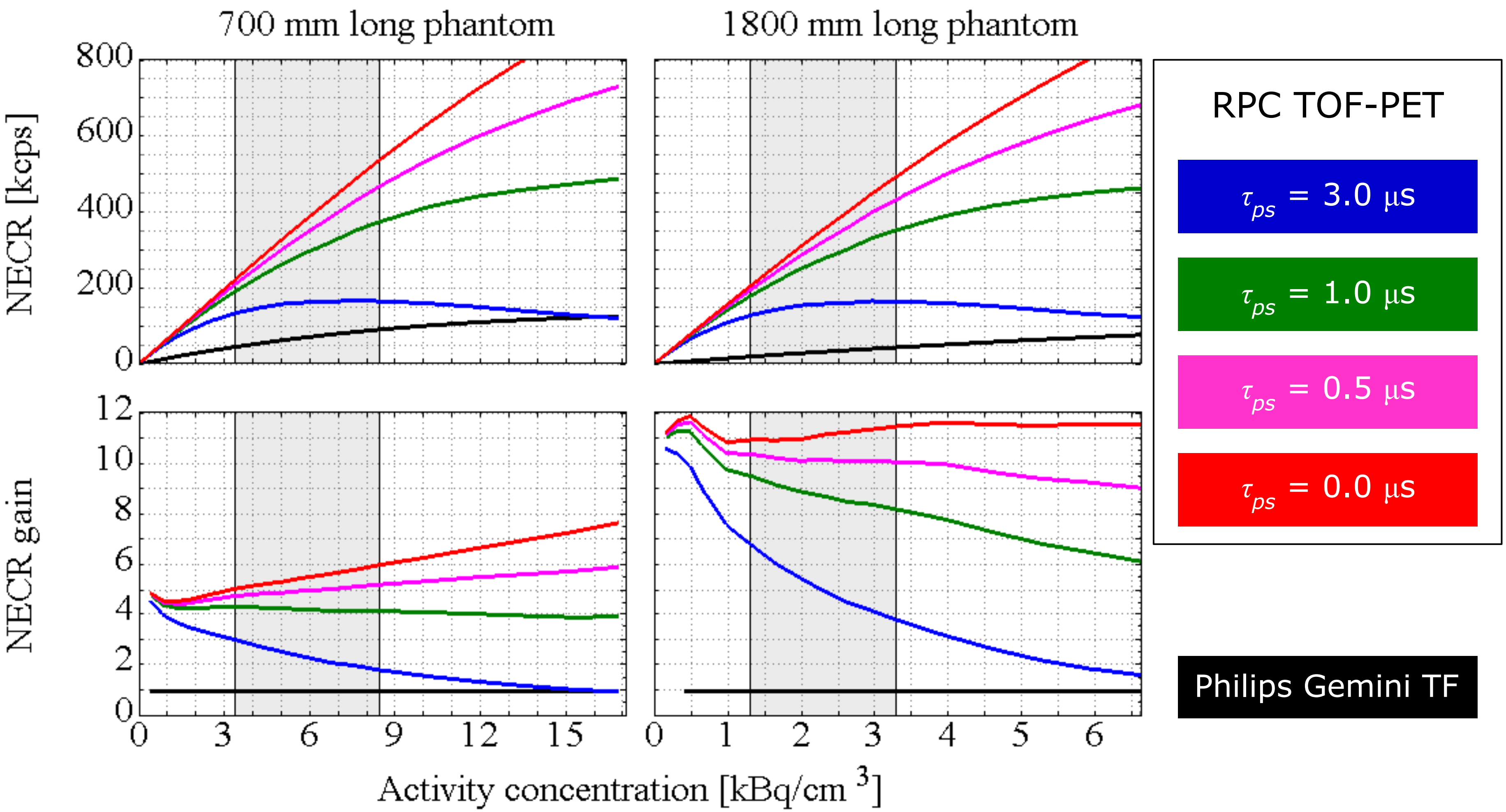

[M.Couceiro et al.,

Full TOF-PET System for Mice: Geometry

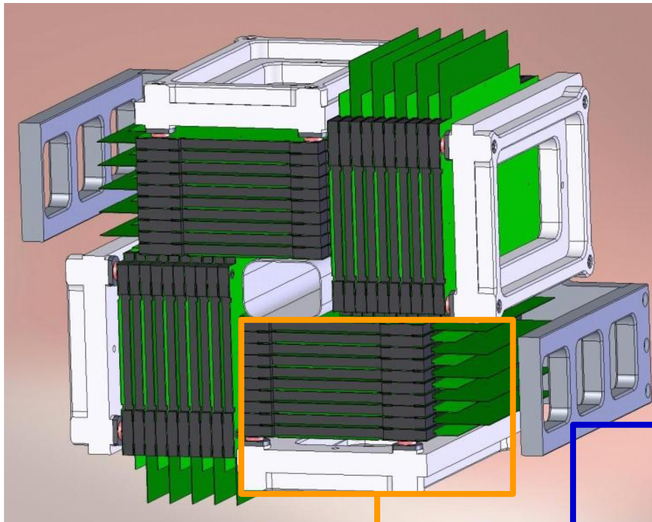

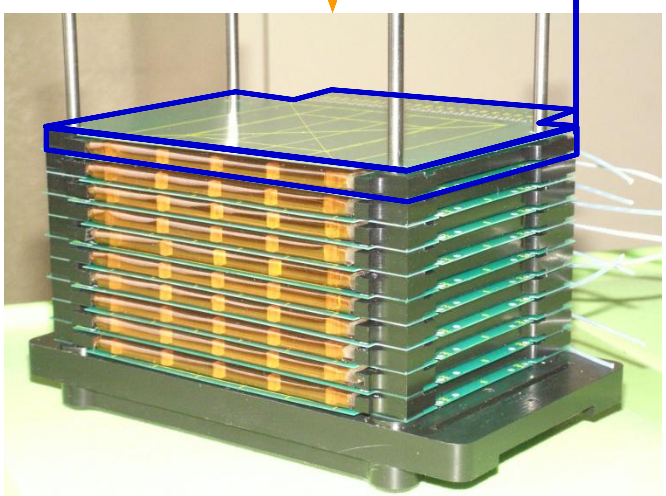

5×0.35 mm gaps; 6×0.38mm glasses; ~5 mm thick

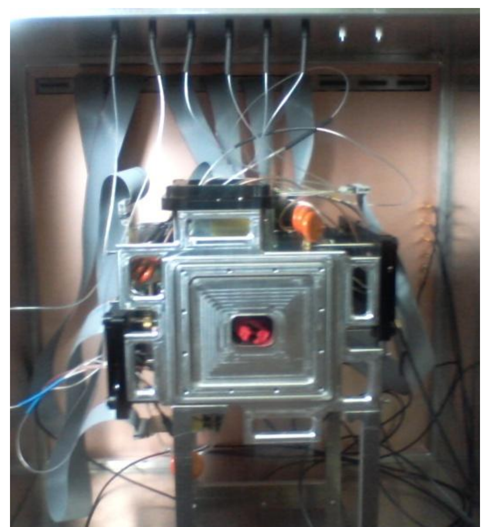

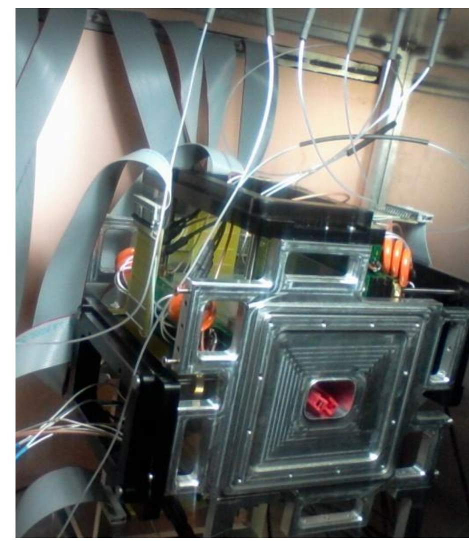

Full TOF-PET System for Mice: DAQ

a. **Scanner Geometry**

192 charge amplifiers optimized for large Cin

192 channels 12 bit streaming ADC

Digital Pulse Processing by software

Few channels of 100ps TDC also used

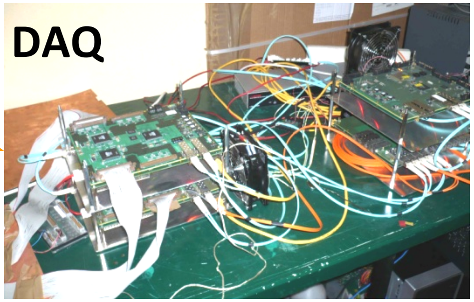

Provided by the HADES DAQ group
GSI, IKF (Germany) and JU (Poland)

TOF-PET for Mice: Experimental Resolution

- Full area, all angles (up to 56º), all gaps (DOI resolution).
- Joint reconstruction of the source (0.2 mm diameter) in 2 positions separated by 1mm.
- ~130k LORs in 3.5M 25μm voxels, MLEM reconstruction.
- Color maps: planar profiles including peak density point.
- Isosurfaces: 50% relative activity.

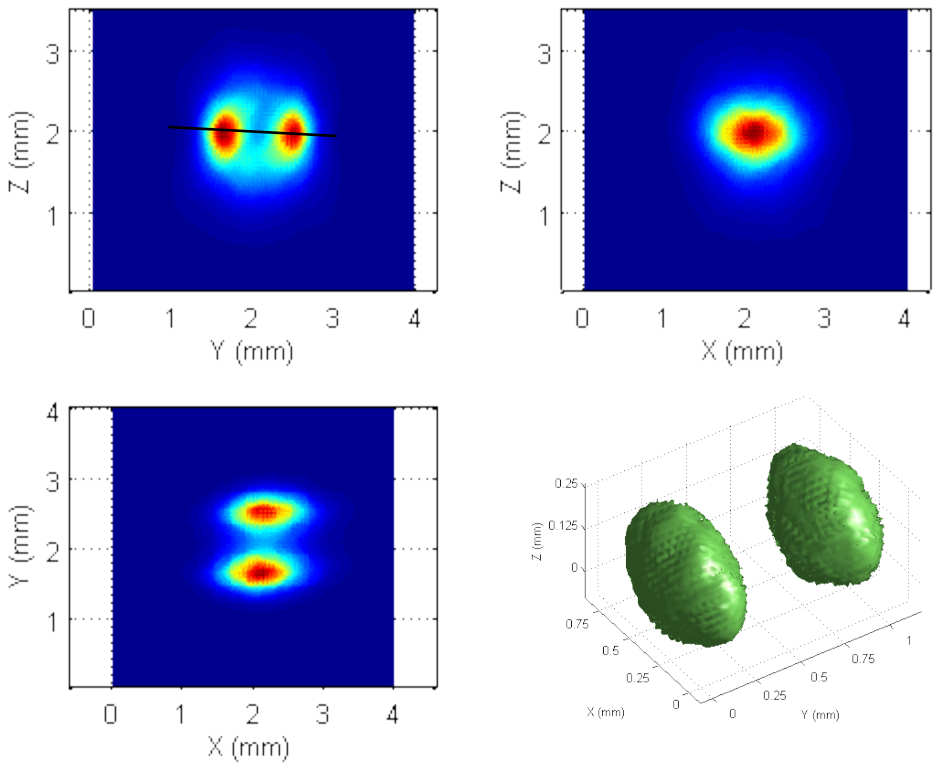

- Activity profile modeled as two point sources + background
- Estimated Resolution **~0.4mm**

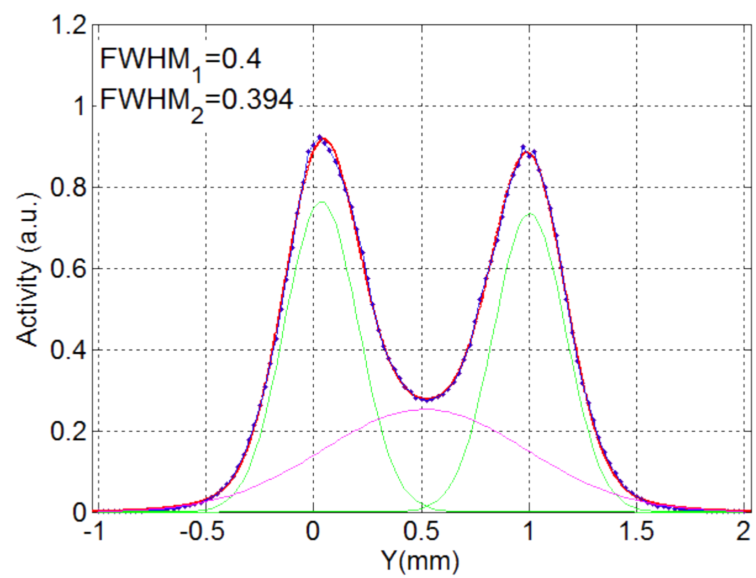

P. Martins et al.,

Preliminary Images of mice (obtained at ICNAS)



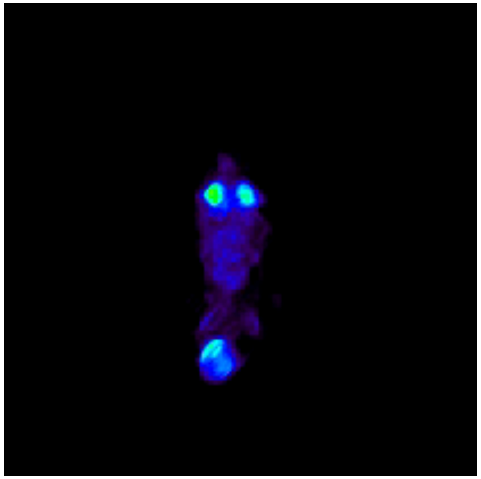

Poor animal resting after FDG injection and in the scanner tunnel
(The head is central and the heart is at the edge of the field-of-view)

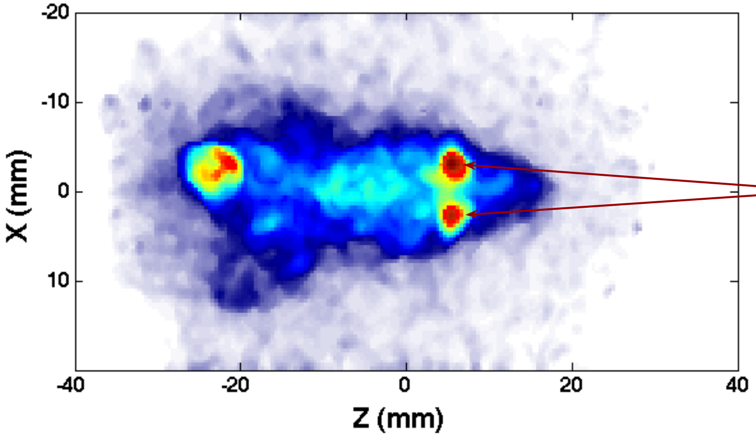

- Maximum intensity projection.
- The two hot spots in the head are likely the Harderian glands.
- The heart walls seem resolved.

Preliminary Images of mice (obtained at ICNAS)

Images of a mouse for 60 minutes acquisition with the preclinical RPC-PET prototype after injection of 3.6 MBq of FDG, and 30 minutes of resting.

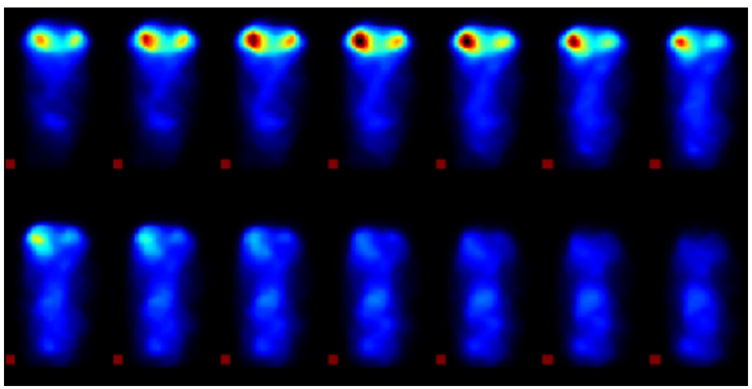

Coronal slices of the head, depicting what are probably the Harerian glands; (b) Axial slices of the heart.

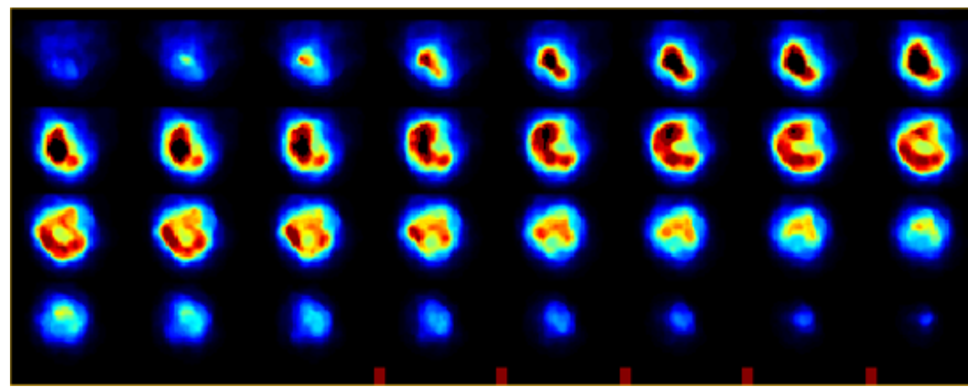

Axial slices of the heart.

Preliminary Images of mice (obtained at ICNAS)

Images of a mouse for 90 minutes acquisition with the preclinical RPC-PET prototype after injection of 15.6 MBq o ^{11}C-Raclopride

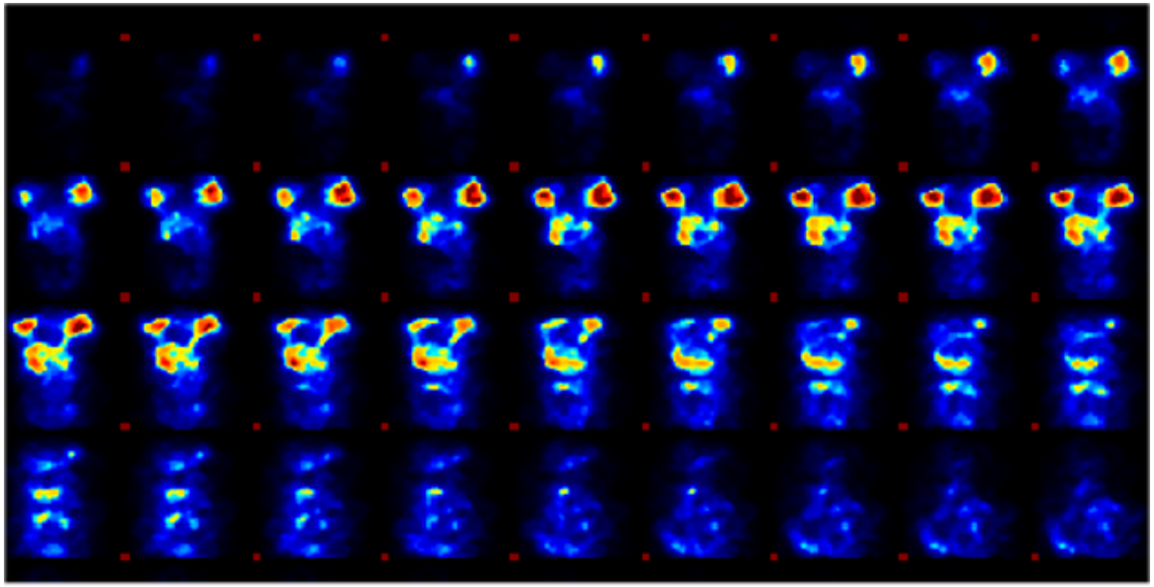

Coronal slices

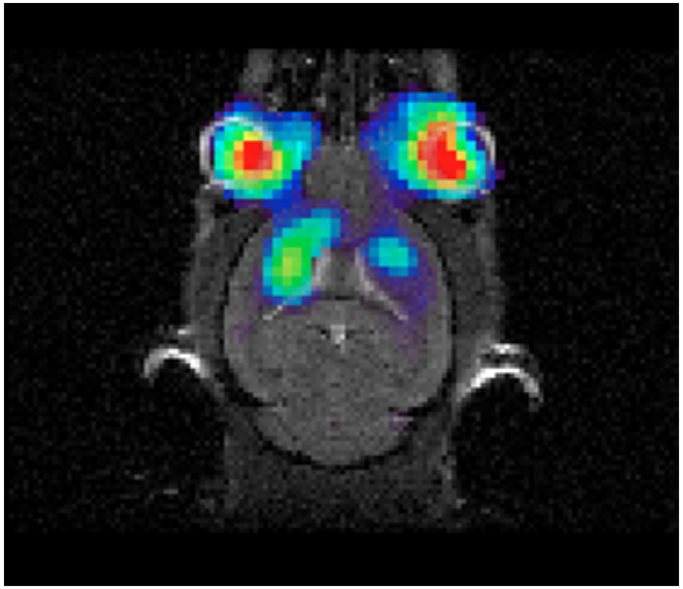

A coronal slice of PET/MRI image fusion

Currently: test of readout electronics

- 21 charge channel
- 32 time channels

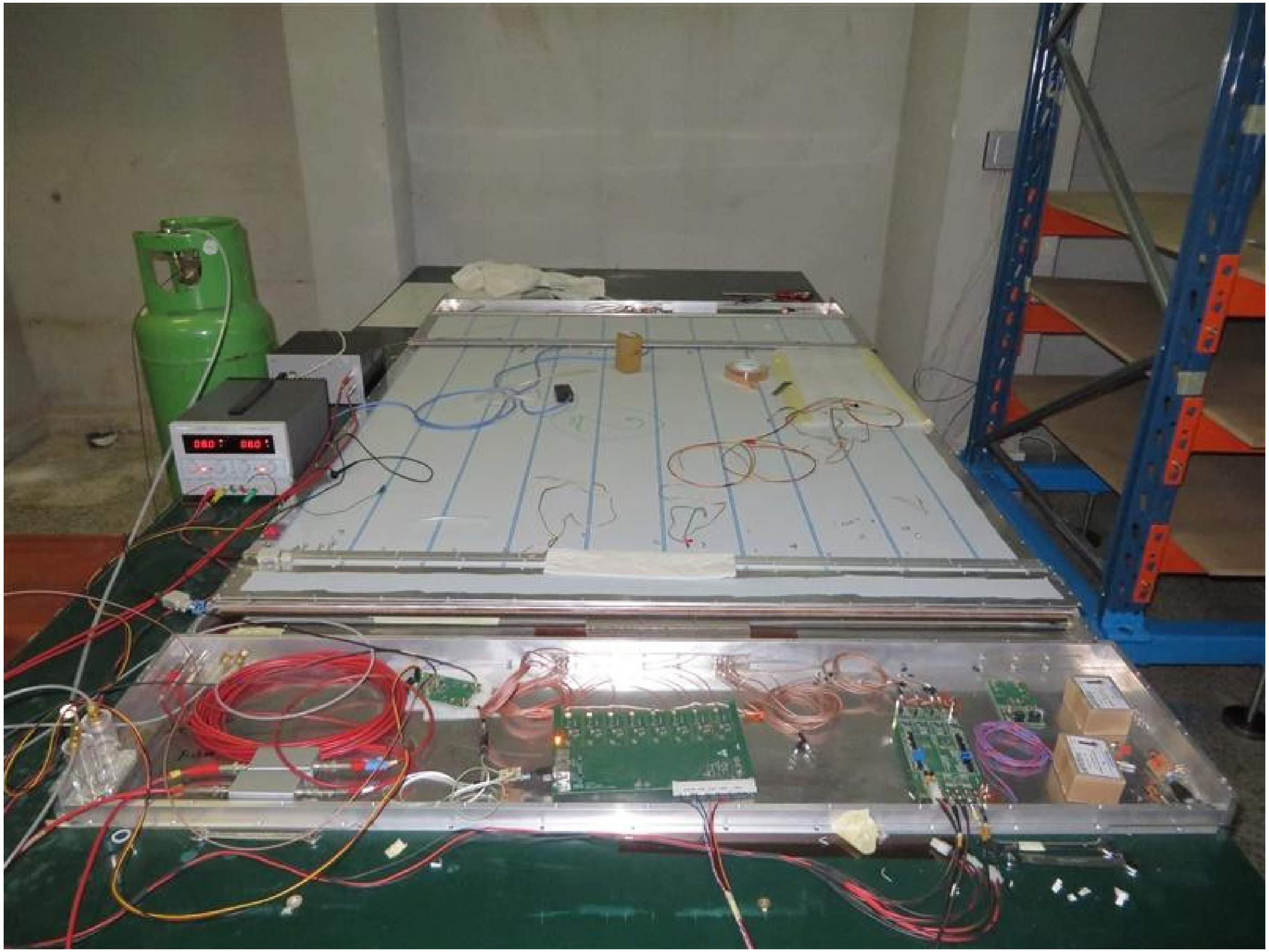

RPC-PET: Outlook

- Animal RPC-PET
  - Number of RPCs/head will be extended from 3 to 7 (out of a maximum of 10), in principle quadrupling the sensitivity.
  - A new version of the front-end electronics will be developed, trying to minimize the digital noise induced by the ADCs into the trigger system, which considerabl reduces the sensitivity of the scanner.
- Human RPC-PET
  - Test of the readout system started in 2014 will be completed
  - Development of a realistic RPCs and (very thin) electrodes, aiming at a first full-body scanner prototype.

Detectors and Monte Carlo in Medical Physics

Development of Plastic Scintillator Dosimeter (PSD) for radiology

BC-404 (PVT) 8 mm / 3mm Ø
BCF-60 (polystyrene) 10 mm / 3 mm Ø

Signal collected by a PMMA optical cable

PMT Hamamatsu R647P
Single channel reading

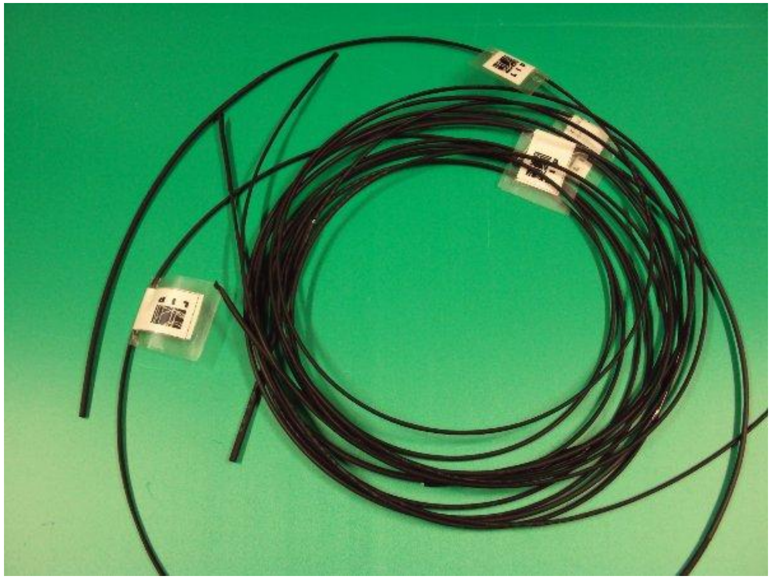

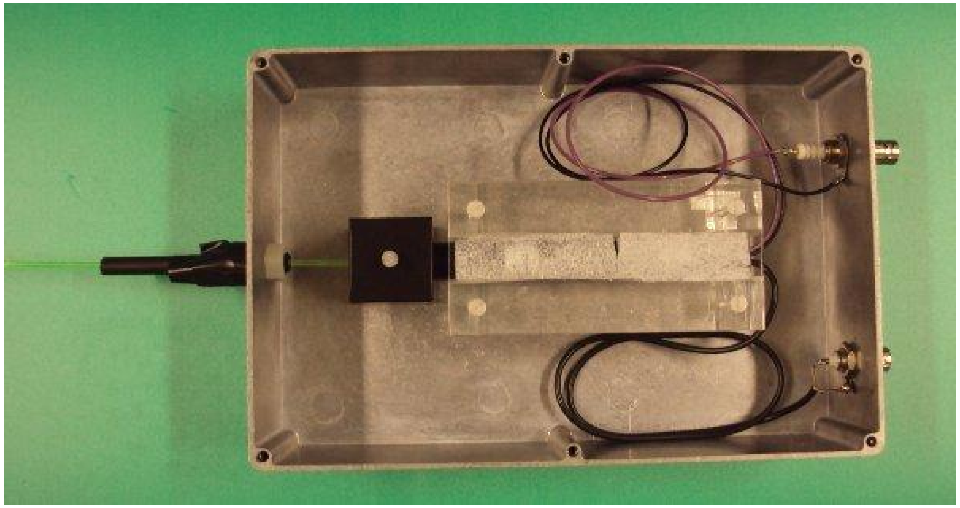

Detectors and Monte Carlo in Medical Physics

Hospital da Luz, Lisboa
Siemens Mammomat
Breast Tomosynthesis

Dose study with PMMA breast slice phantom

Farmer chamber

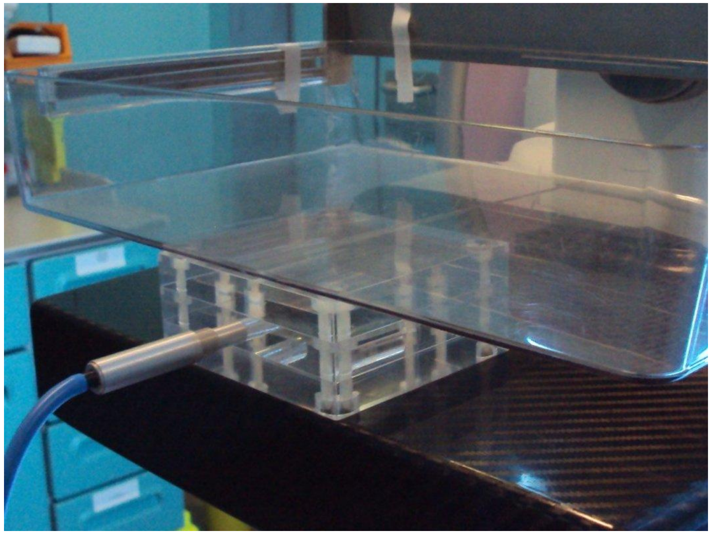

Plastic scintillator dosimeter

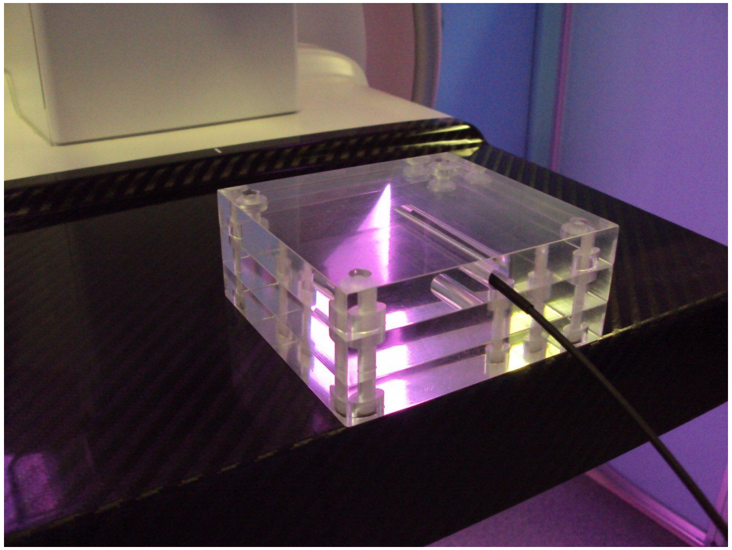

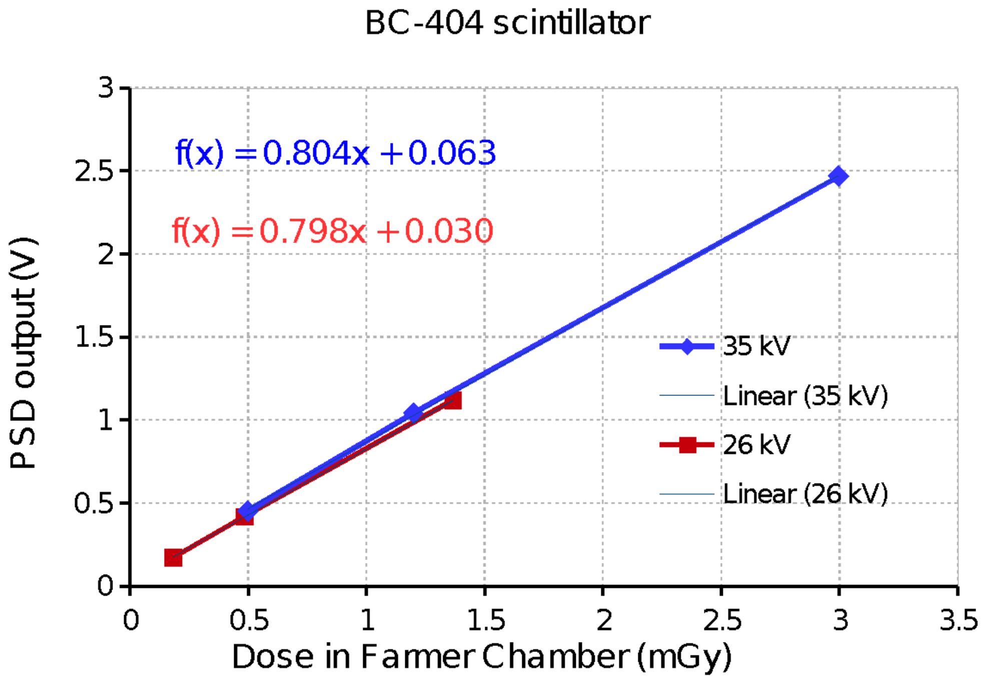

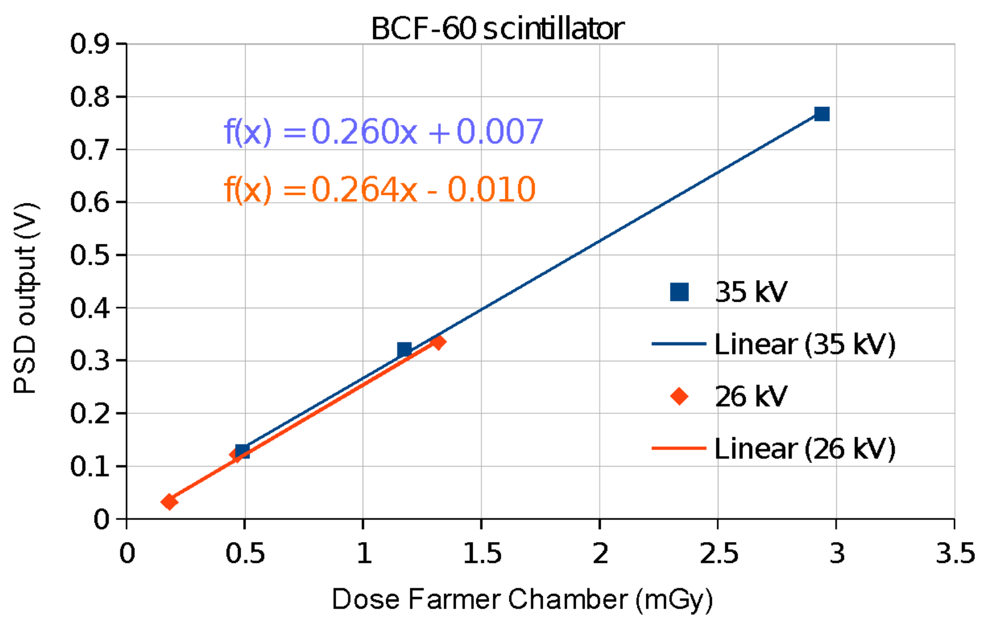

Better linearity and signal output with BC-404 scintillator

Detectors and Monte Carlo in Medical Physics

Full Siemens Mammomat MC simulation

Good agreement between Penelope MC simulation and hospital measurements

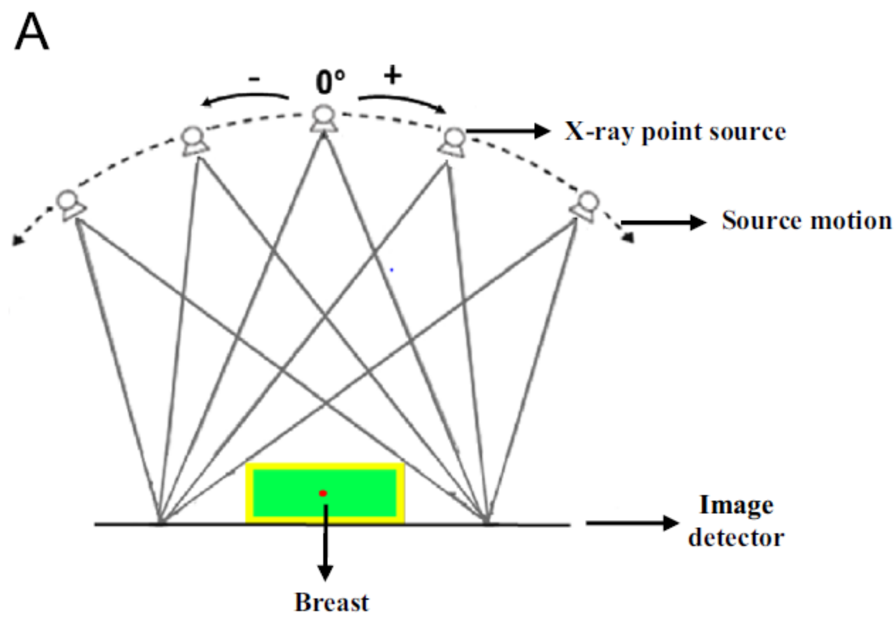

The tomograph head rotates 50º each acquisition. (figure From M. Baptista et al., Rad. Phys. Chem. 104 (2014) 158-162)

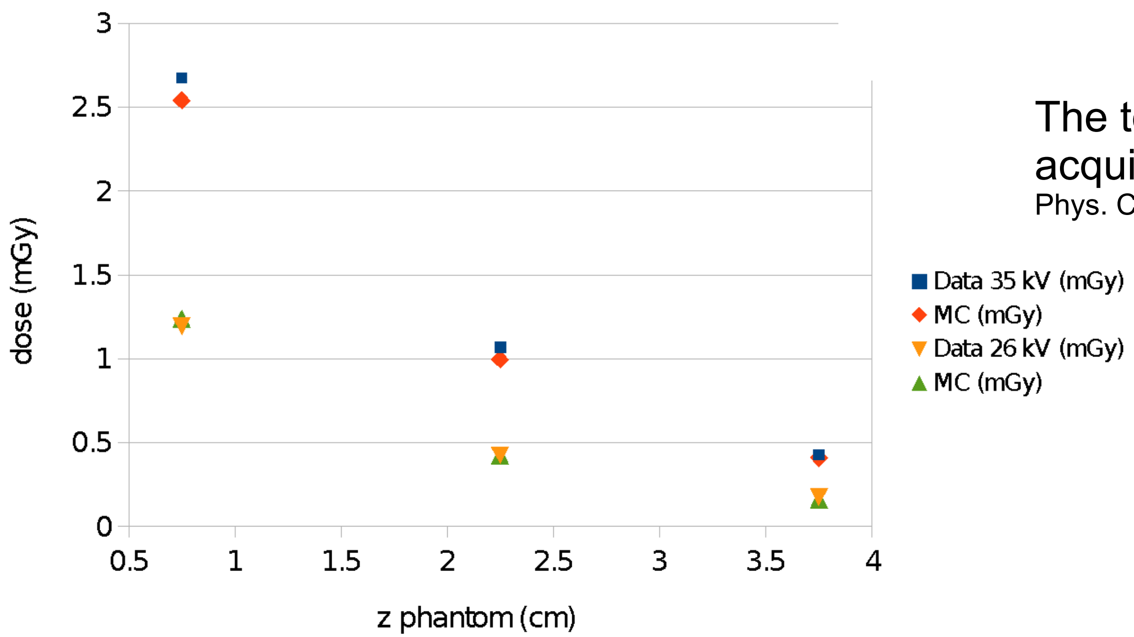

Laboratory for the Study of Radon Exposure Effects

(Uni. Beira Interior, Covilhã)

New lab equipped for laboratory and field analyses

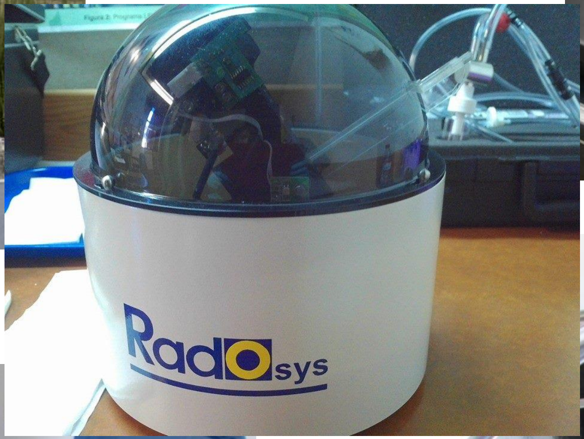

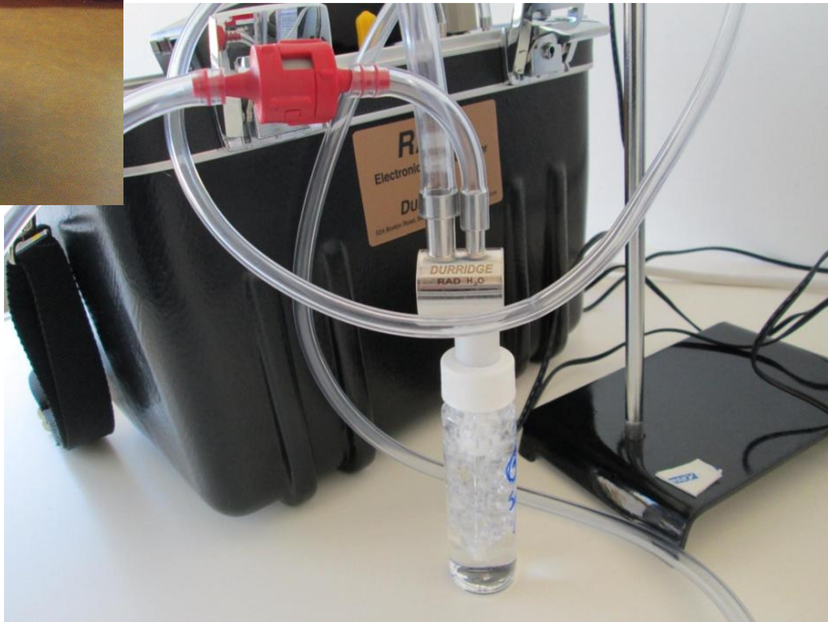

Detectors and Monte Carlo in Medical Physics

Research on population risks due to radon exposition including:

- Monitoring of radon in air, soil and water
- Population survey on lifestyle, diseases and environmental factors

The Covilhã region has high levels of natural radioactivity, where uranium mining was carried out until a few years ago.

Example of water analyses in public water distribution (RP) and several private water springs.

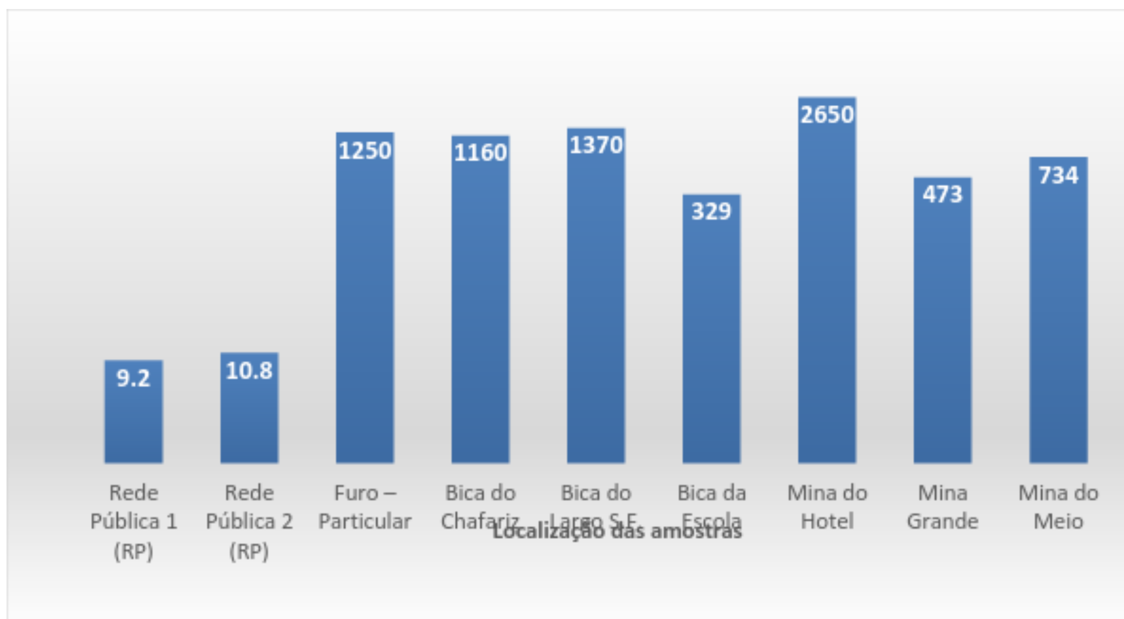

OrthoCT - Orthogonal Ray Imaging for Radiotherapy Improvement

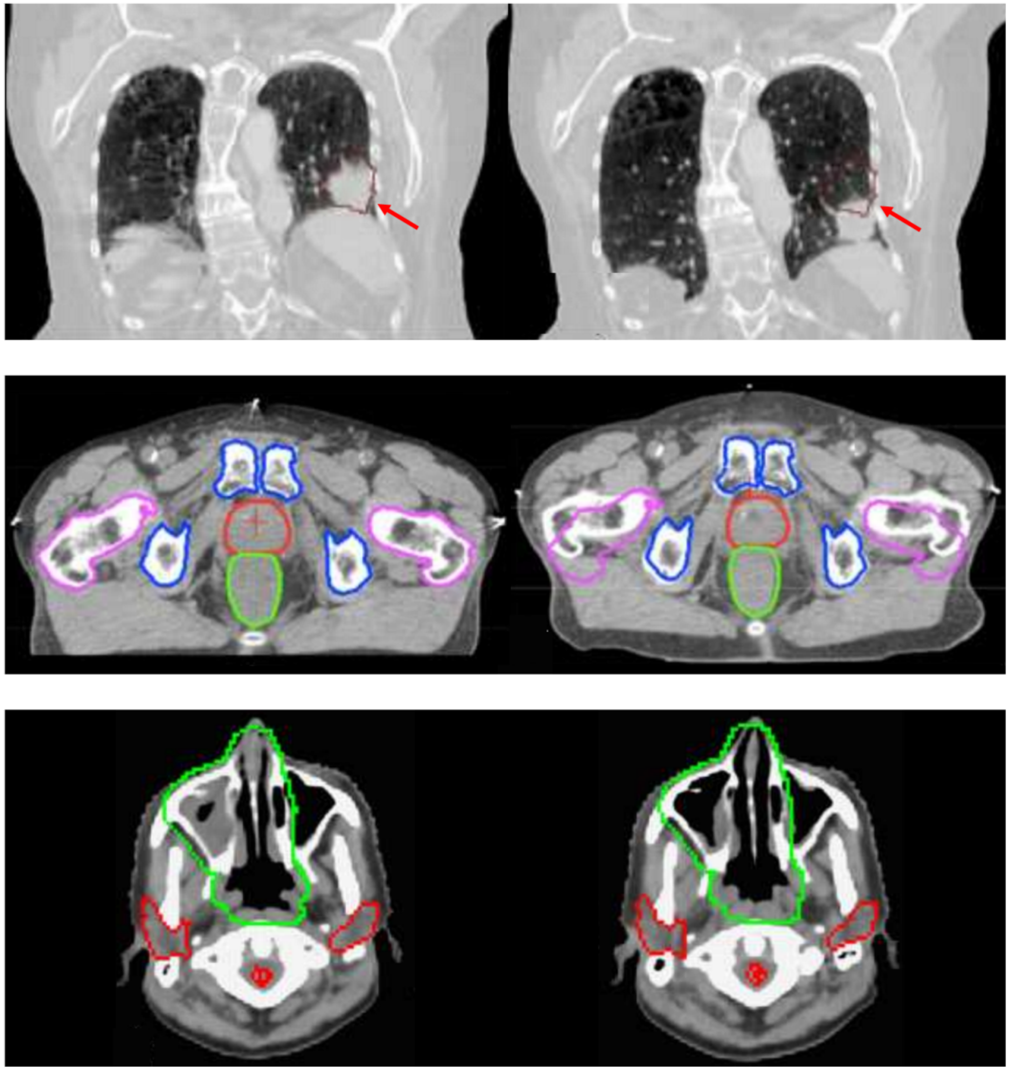

Engelsman & Bert 2011

OrthoCT concept

The scattered radiation that escapes the patient at right angles in respect to the incident beam direction is correlated with its morphological structure and maybe with the dose (ongoing work)

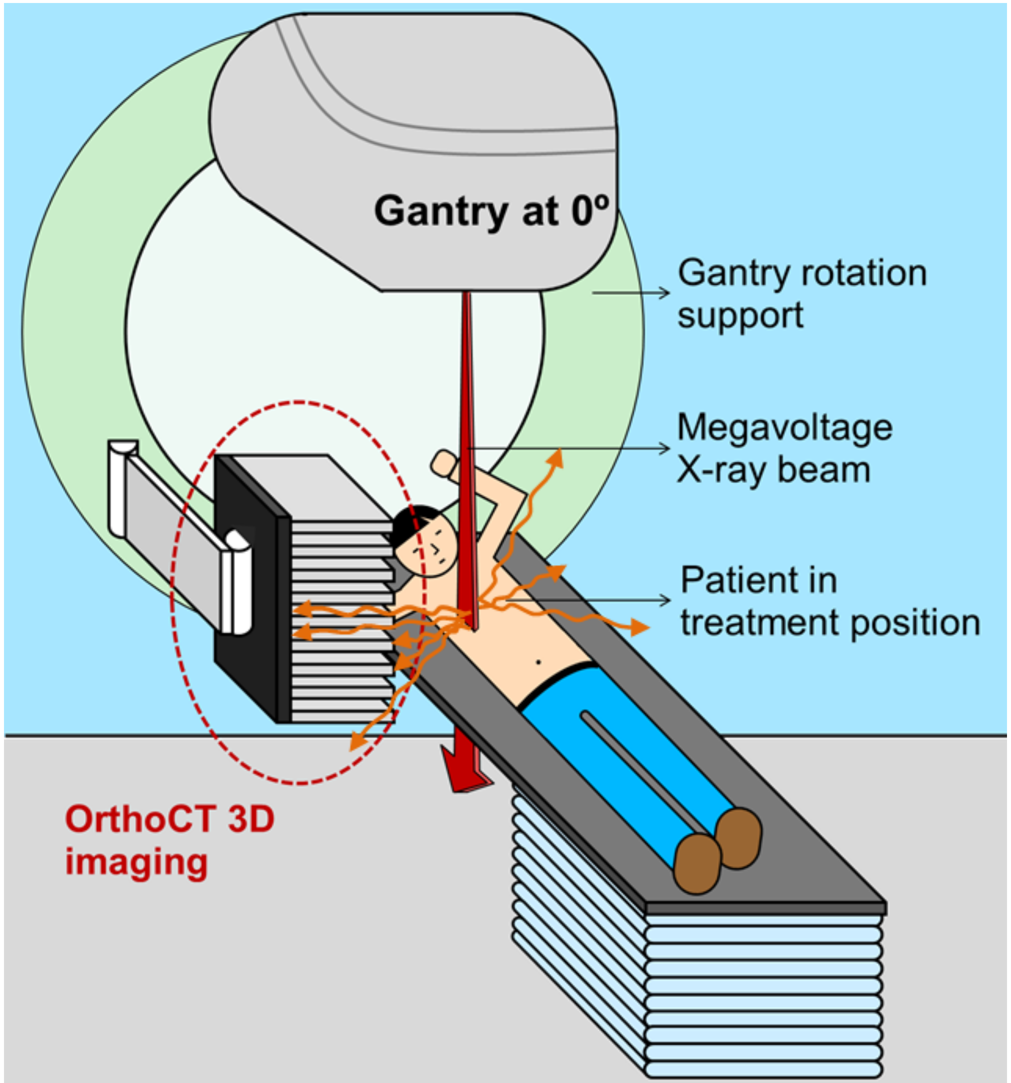

- **3D imaging: a pencil-like photon beam traverses the patient at known (2D) coordinates; the detector slice hit by an emerging photon yields the 3rd coordinate**
- **Rotation-free technique**
- **Scan area can be limited to the tumor only: organs at risk with minimal to null dose exposure**
- **Allows for targeted on-board imaging with low dose**

Simulation study: OrthoCT in lung irradiation

- Simulations with Geant4
- Anthropomorphic phantom (Paul Segars) was adapted into Geant4

Simulated dose distributions

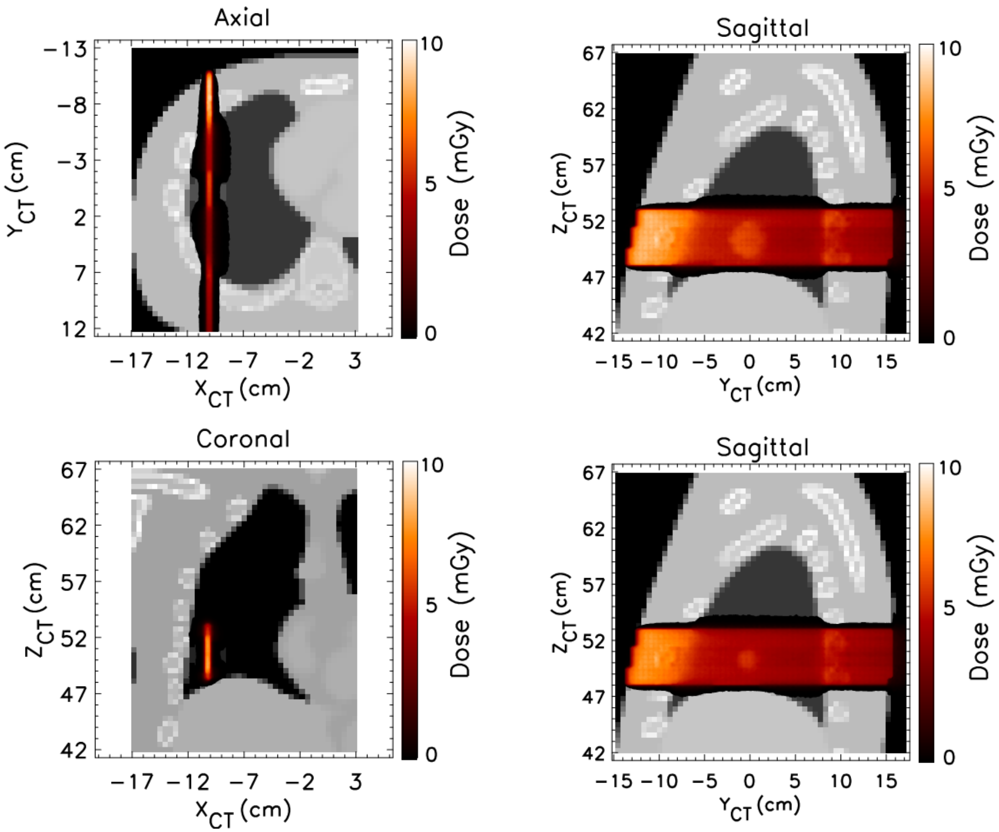

Maximum simulated dose: 10 mGy (ribs)

OrthoCT image

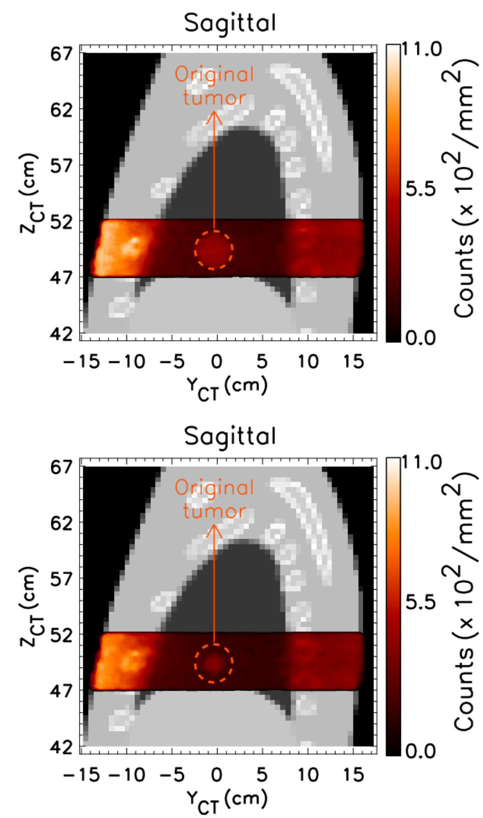

"Original" tumor

Tumor regression

Mathematical collimation

- Acceptance angle: $\theta_X \leq 0.9^{\circ}$
- Photon energy threshold: $E_{\gamma} \geq 250$ keV
- Median filter with a span of 6 píxels

Simulation study: OrthoCT in lung irradiation

Simulation of a full OrthoCT system

(collimator + GSO crystals + photon eletronics readout)

"Original" tumor

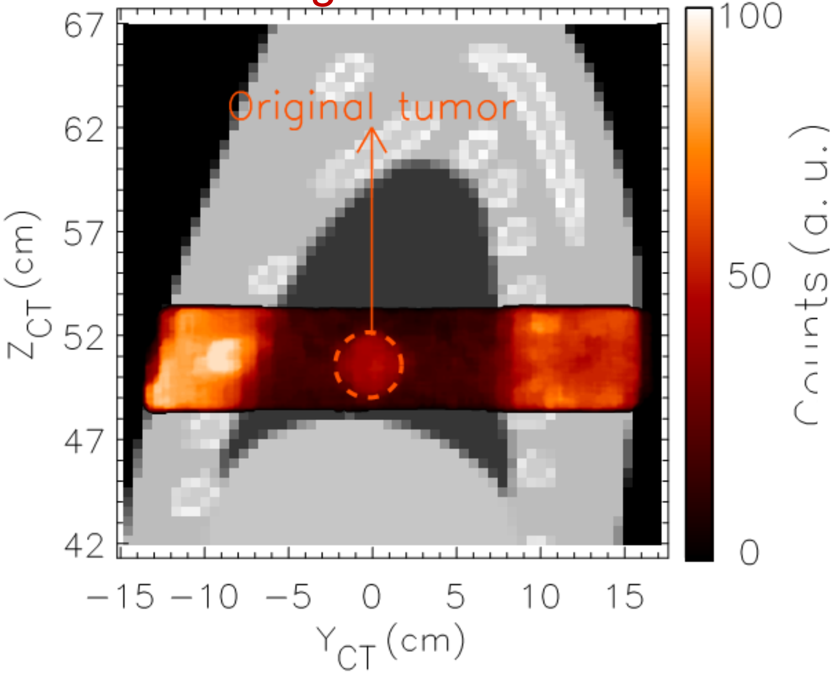

Tumor regression

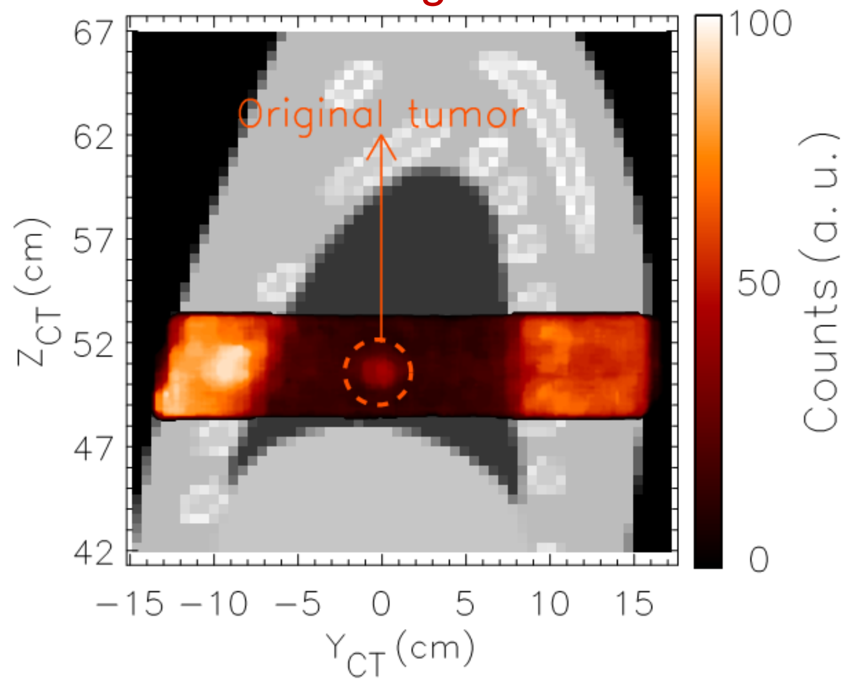

Experimental study: simplified OrthoCT (single pixel) measured in radiotherapy environment

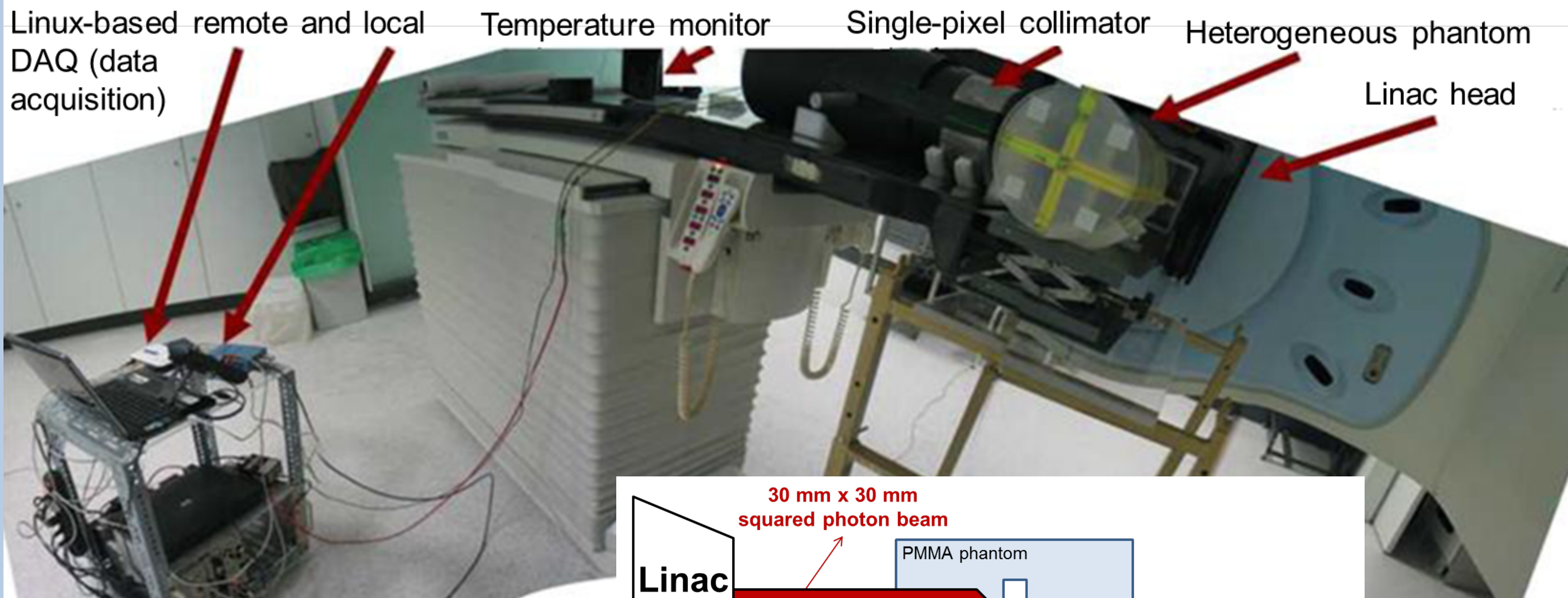

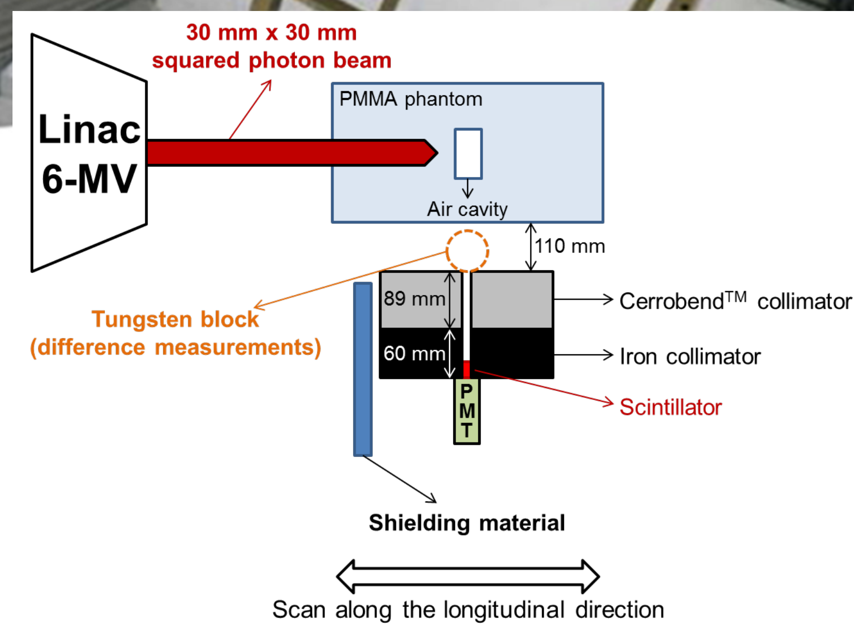

Experimental study: simplified OrthoCT (single pixel) measured in radiotherapy environment

Correlation of *R* = 0.9911 with dose, even in suboptimal conditions

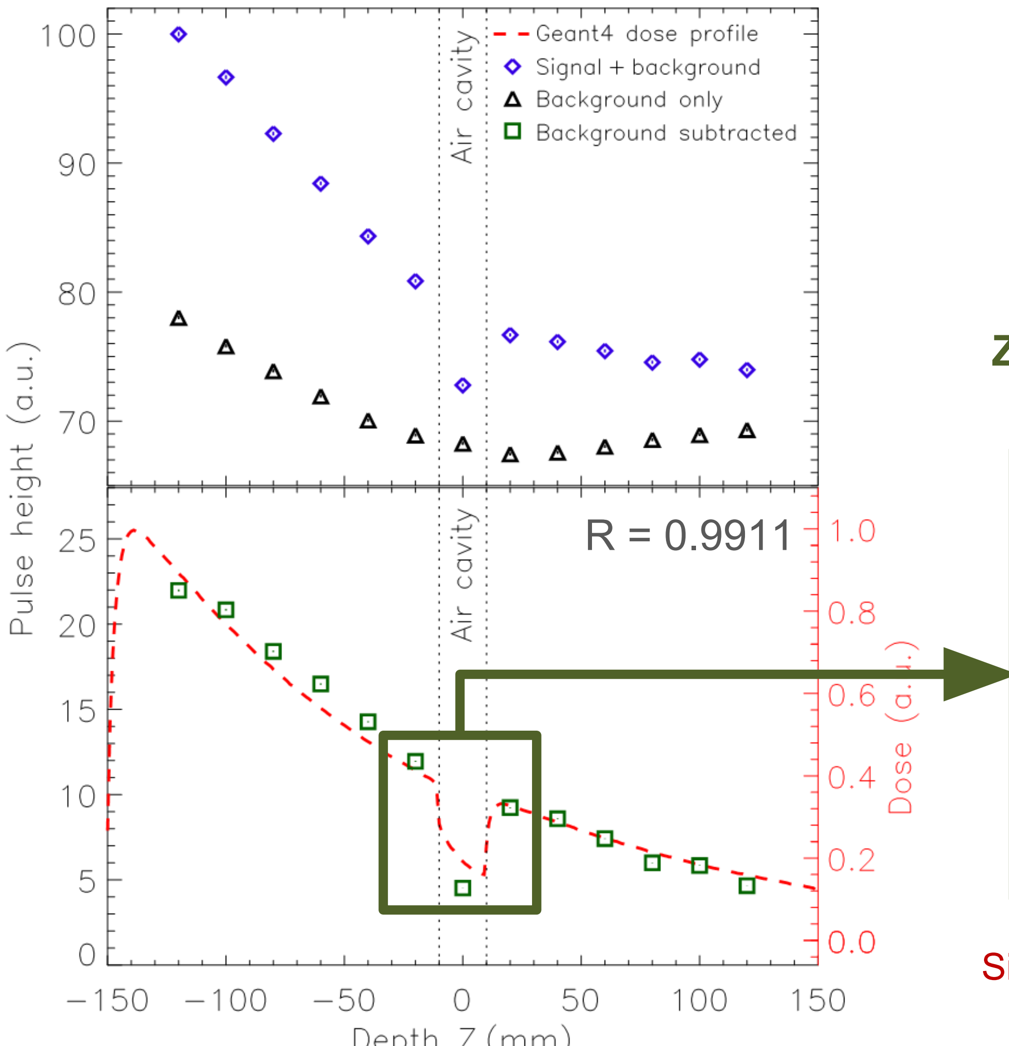

Zoom in of region with air cavity

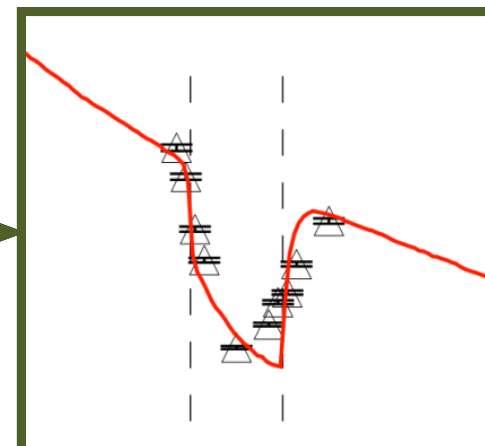

Simões *et al.* 2013

OrthoCT: Plans for 2015 and beyond

Build small-scale prototype OrthoCT detector for in-beam tests

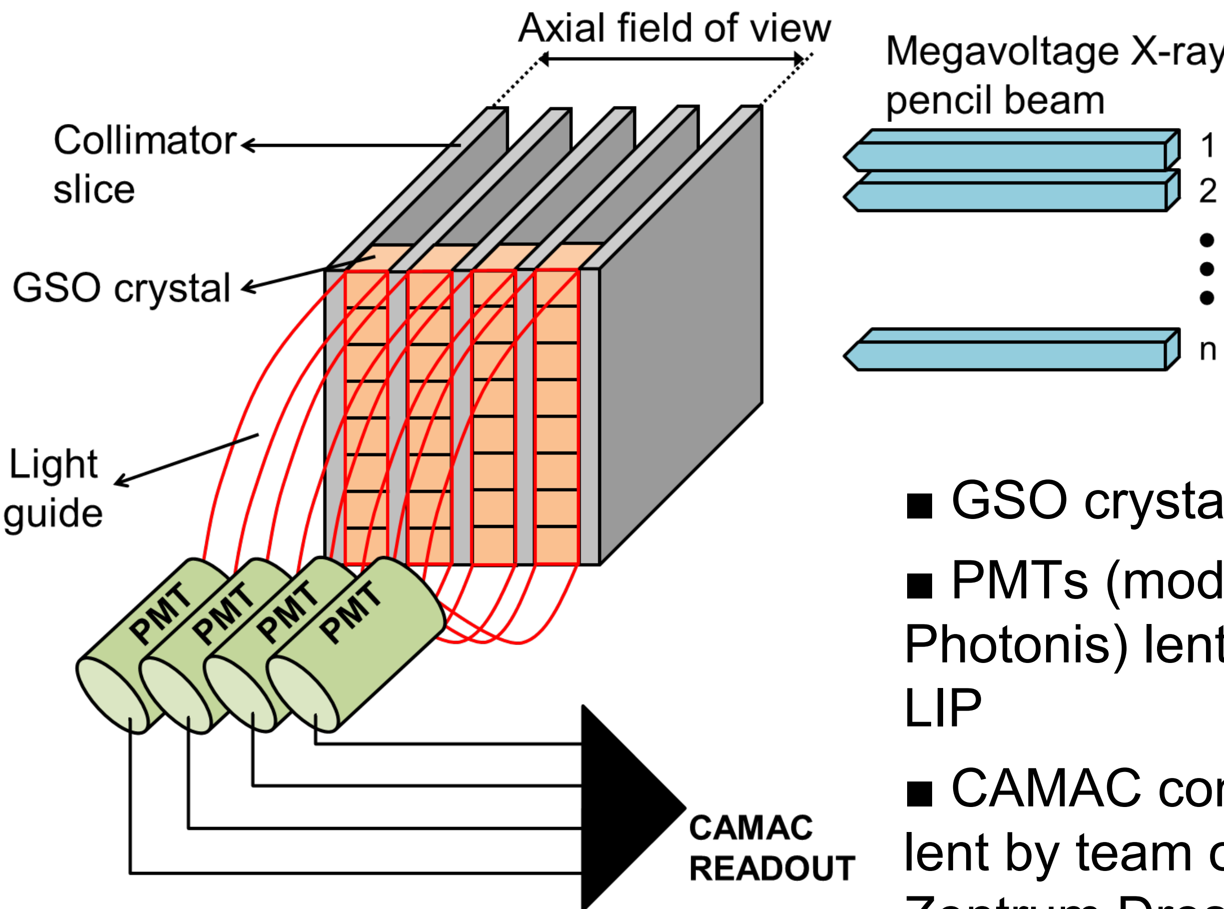

- GSO crystals already at LIP
- PMTs (model XP5602, Photonis) lent by colleague from LIP
- CAMAC controller and DAQ lent by team of HZDR (Helmholtz-Zentrum Dresden-Rossendorf), Germany.

Plans for 2015 and beyond

Test prototype small-scale detector under several radiotherapy beams:

A. **IPO-Coimbra (Coimbra Institute of Oncology): 6 MV beams with flattening filter**

B. **Department of Radiotherapy of Coimbra University Hospital: 4 MV beam with flattening filter**

C. **IPO-Porto (Porto Institute of Oncology): several MV beams each FFF (flattening-filter free)**

Contact multinational radiotherapy machine manufacturers exploring potential synergies

GAMMA - Adaptive Methods for Medical Imaging

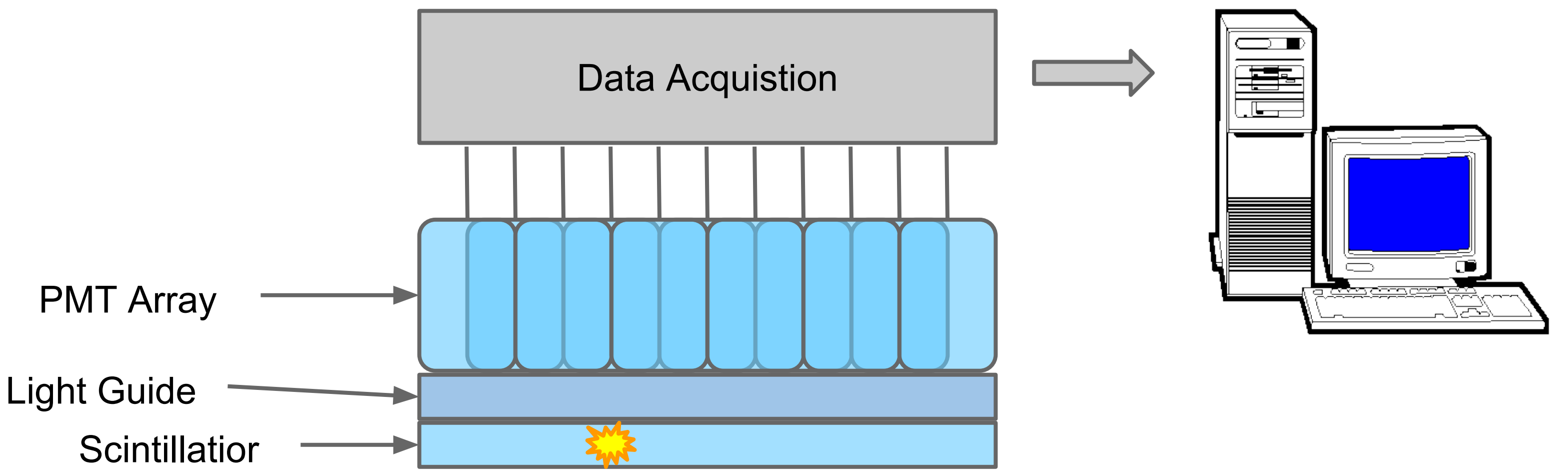

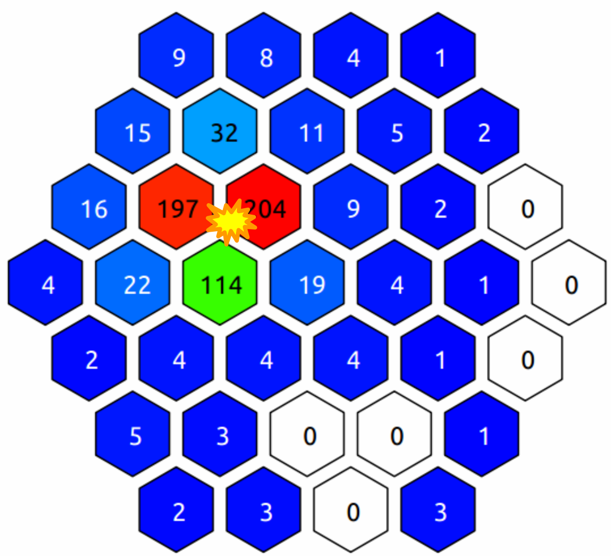

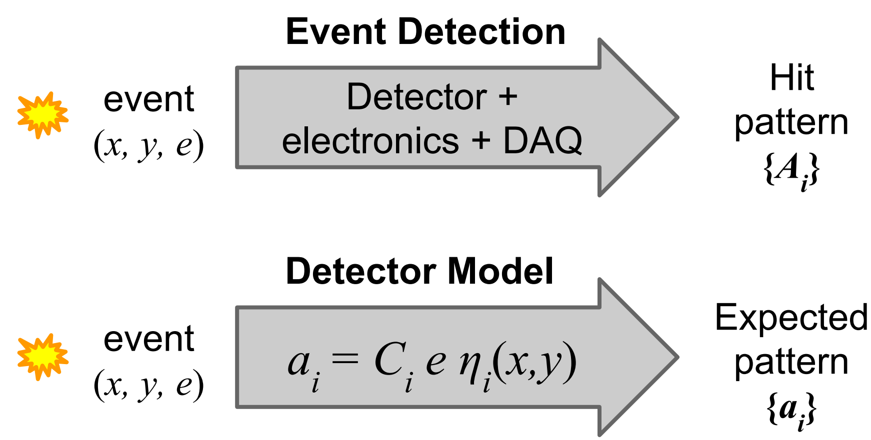

To reconstruct an event from a hit pattern, find x, y and e for which the expected pattern $\{a_i\}$ is in the best agreement with hit pattern $\{A_i\}$.

Light Response Functions

How to find this best match?

- Maximum likelihood (Gray & Macovsky, 1976)
- Least squares
- Artificial neural networks
- Nearest neighbour

Light Response Functions
$\eta_i\,(x,y)$ needed

Light Response Function (LRF) $\eta_i(x,y)$ characterizes response of a PMT as a function of light source position (x,y). LRFs can be obtained from:

- **Direct measurements** (time consuming and expensive)
- **Simulations** (requires detailed knowledge of detector geometry, material optical properties and PMT properties)
- **Iterative Reconstruction** from flood irradiation data

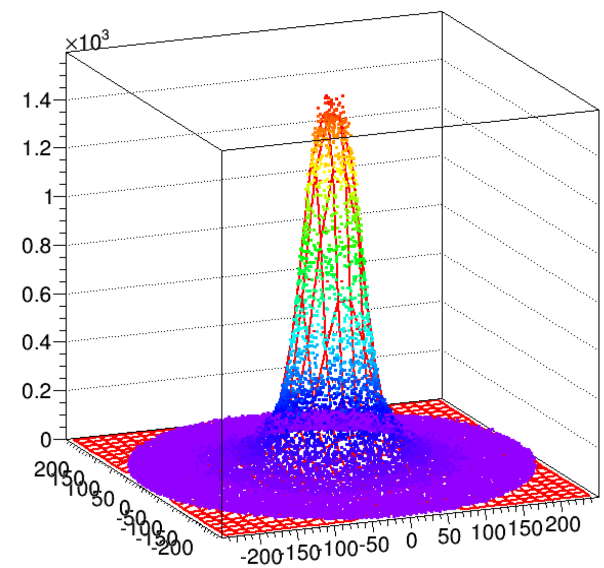

Iterative LRF reconstruction

This technique was invented in LIP during work on ZEPLIN-III project

1. Chose a 1st approximation for LRFs (e.g. from simulation)
2. Reconstruct the event positions using the LRFs
3. Use the reconstructed event positions to update the LRFs
4. GOTO 2

The first objective in this study was to veryfy that the approach developed for much higher photon statistics (10^5 per event) will continue to work for a gamma camera (4000 phe per

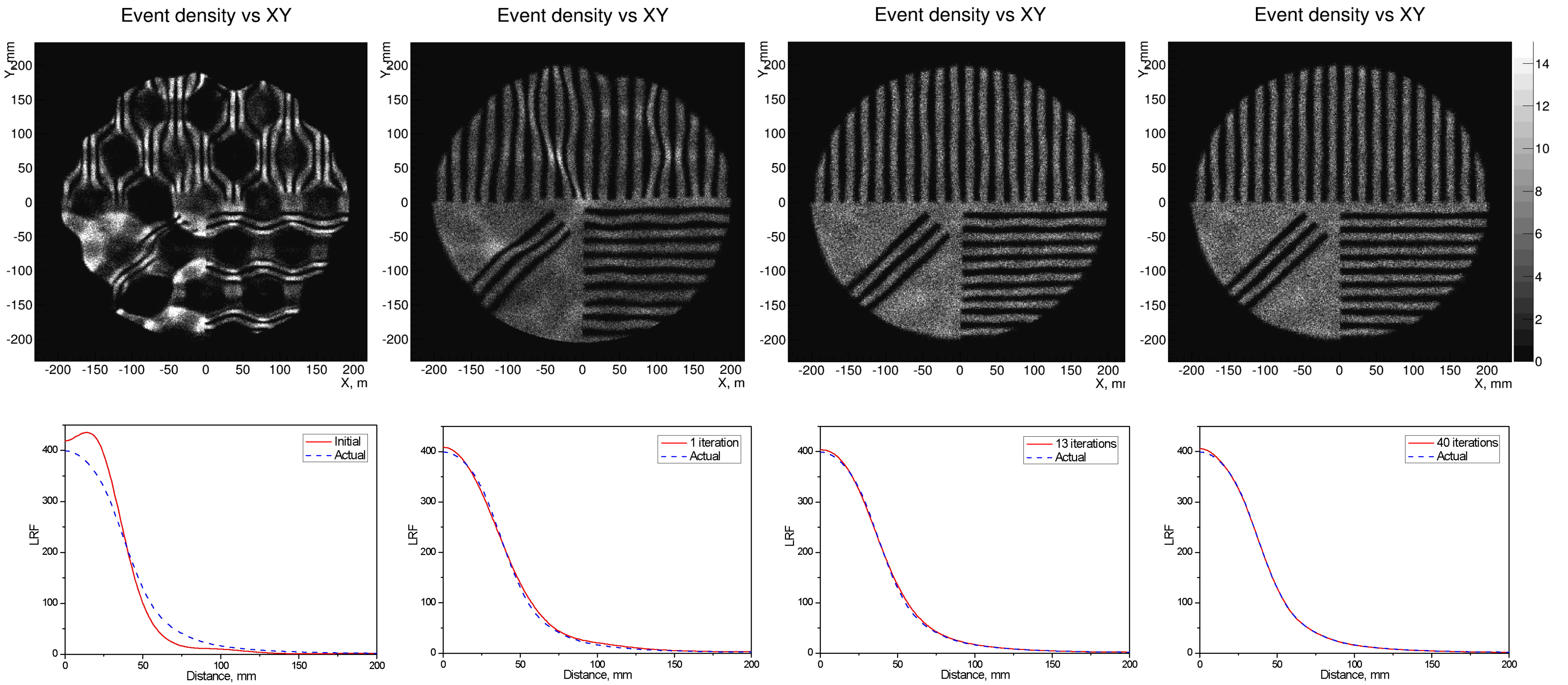

Initial guess | 1 iteration | 13 iterations | 40 iterations

Commercial gamma camera upgrade

A decommissioned commercial gamma camera (GE Maxicamera 400T) was retrofitted with a custom multichannel data acquisition system based on MAROC3 front-end ASIC. This allowed readout of individual PMTs required for statistical event reconstruction.

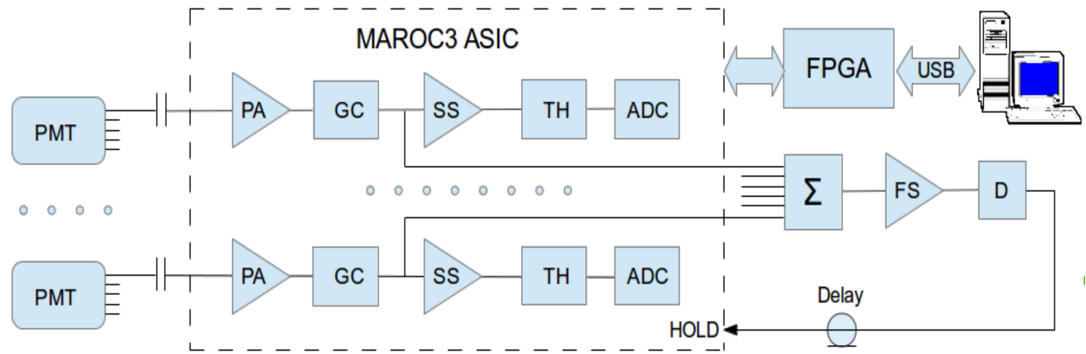

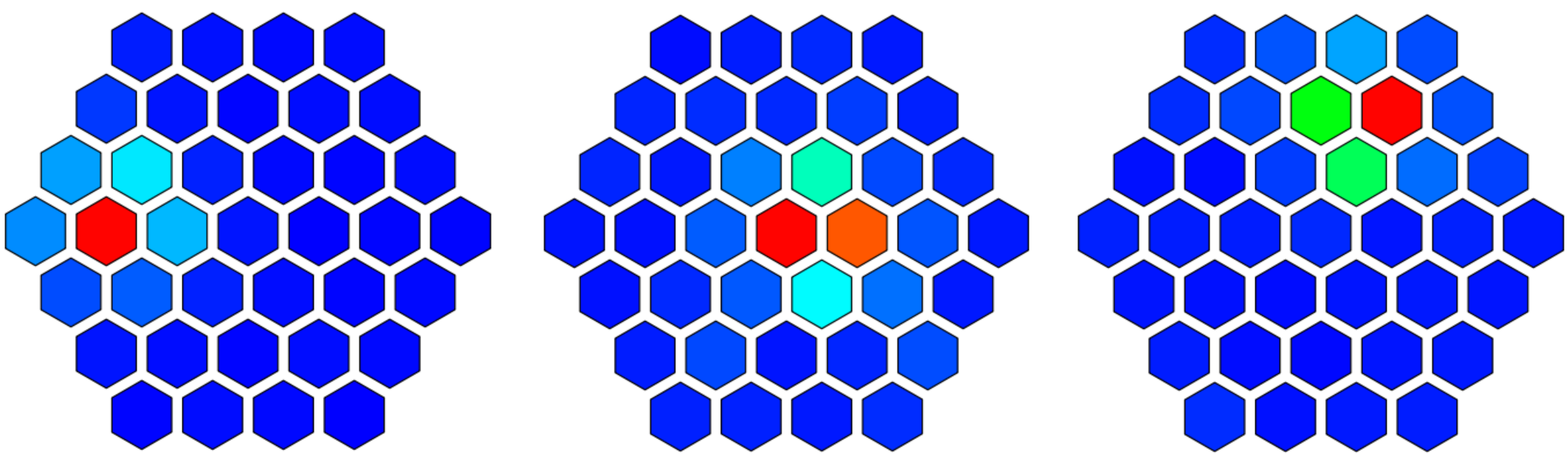

Examples of events acquired with ^{57}Co source (122 or 136 keV)

Commercial gamma camera upgrade

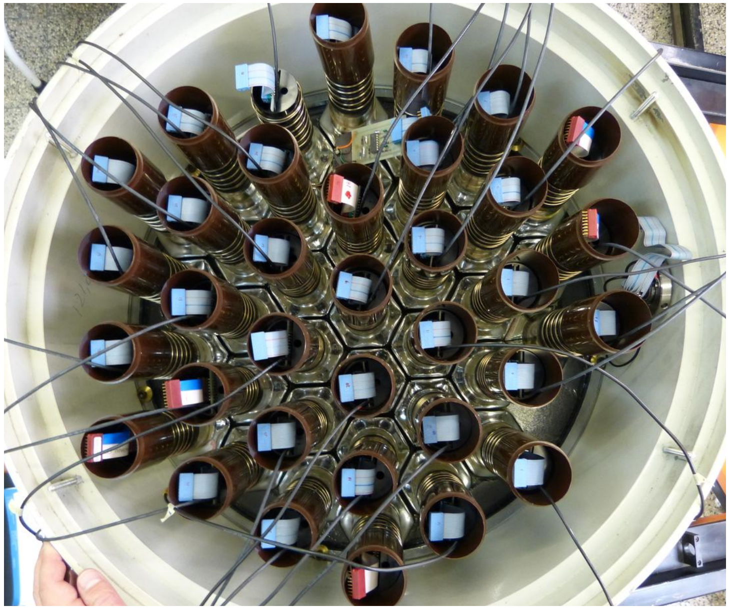

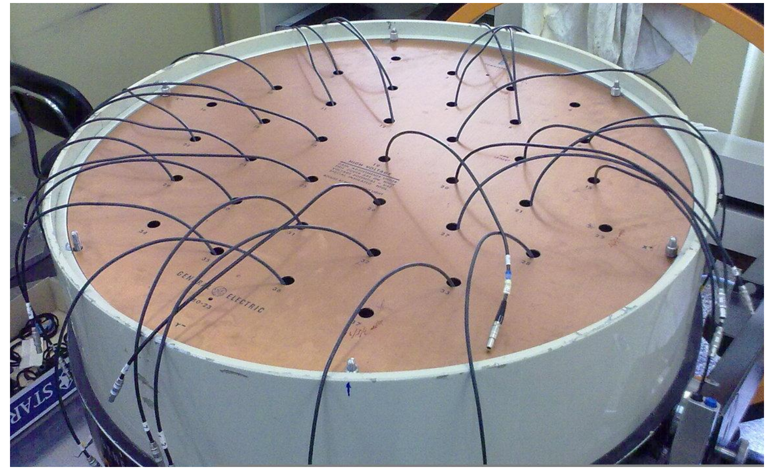

Iterative LRF reconstruction

- The data were recorded with the upgraded camera irradiated by a ^{57}Co source through a 3 mm thick Pb mask.
- Simulated LRFs were used as the initial approximation
- The gains were (roughly) adjusted using an automatic procedure to achieve uniform trigger efficiency. No separate calibration was performed.

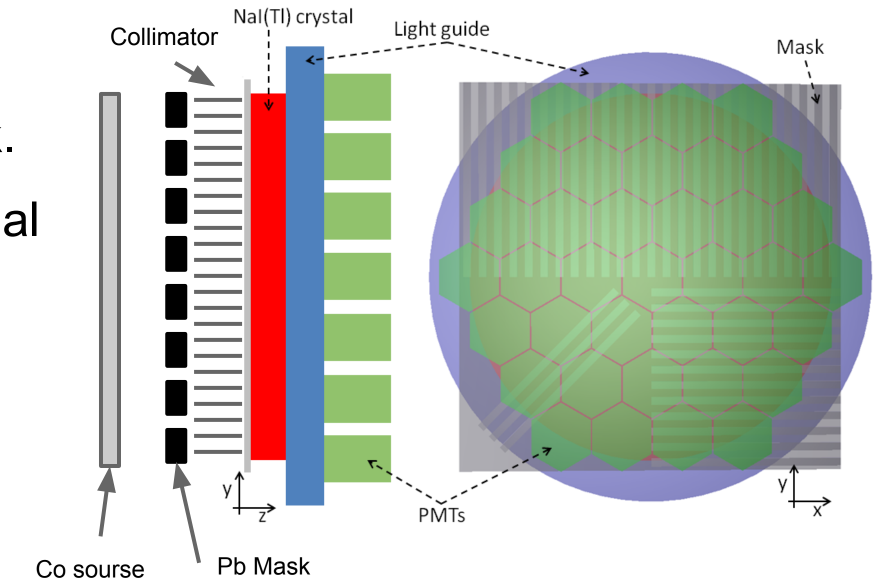

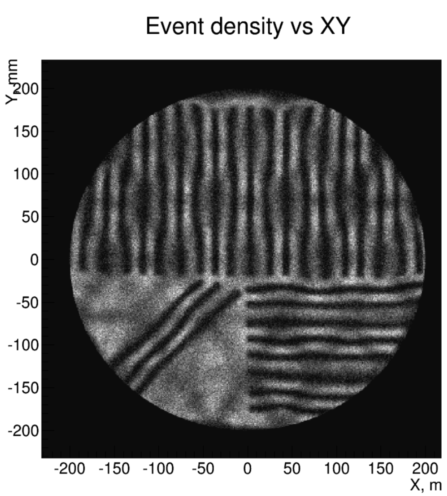

Initial guess

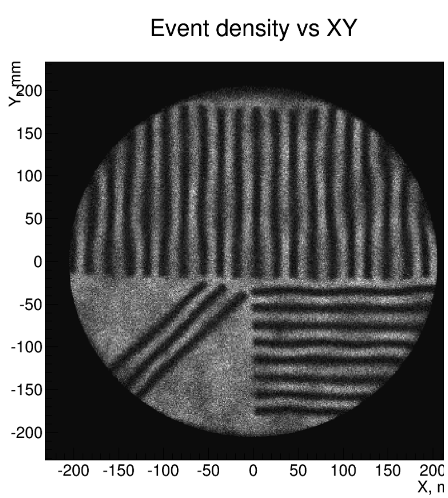

1 iteration

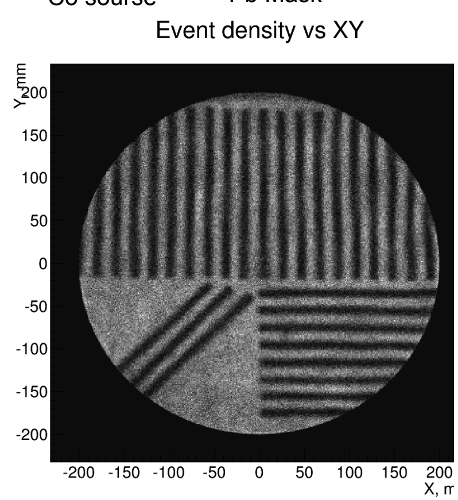

10 iterations

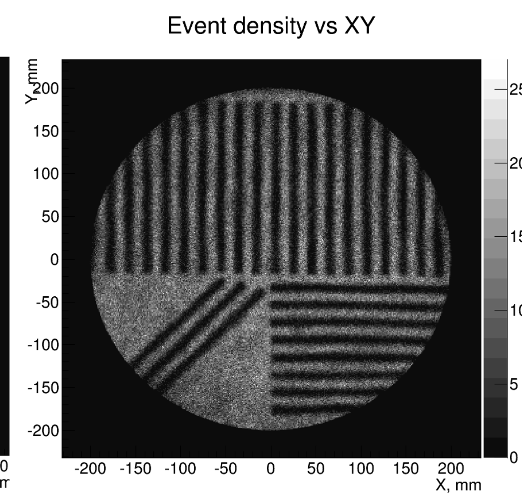

40 iterations

The results will be published soon in *Phys. in Med. Biol.*

Software development

ANTS-II: Integrated software package for position-sensitive scintillation detectors.

Main modules:

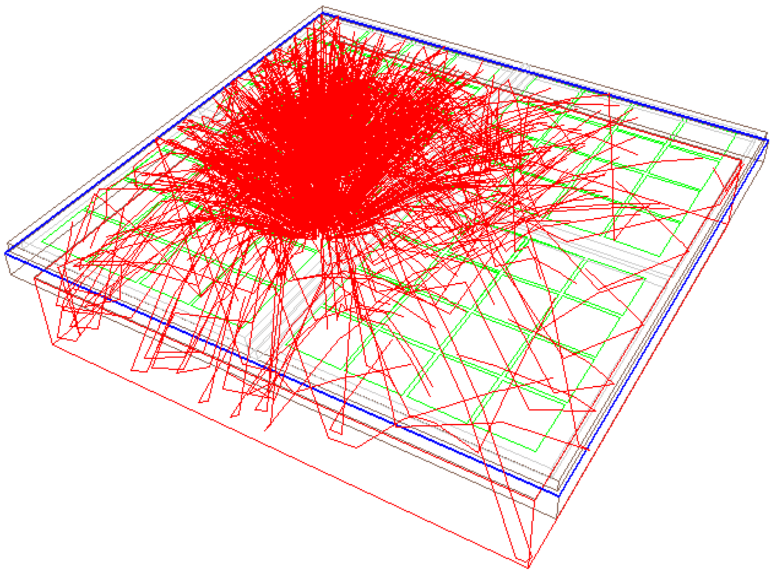

- Detector builder
- Simulator
- Reconstructor
- Data importer and filter
- Data explorer & visualizer
- LRF fitting

Features:

- Wide range of reconstruction algorithms: CoG, ML, LS, contracting grids and neural networks
- Intergrated LRF and gain reconstruction algorithms
- Mutlithreading - perfornance scales with number of CPU cores
- Reconstructon on GPU - up to 10^6 events per second
- Interactive and batch modes, scripting
- Multiplatform, open source

GAMMA: Future development

Work on compact high-resolution gamma camera with SiPM readout:

- Build a new prototype with the light response optimized for self-calibration (simulations are under way)
- Measure camera response and charaterise its performance for 140 keV gamma rays using a well collimated Tc source on XY coordinate table (under construction)

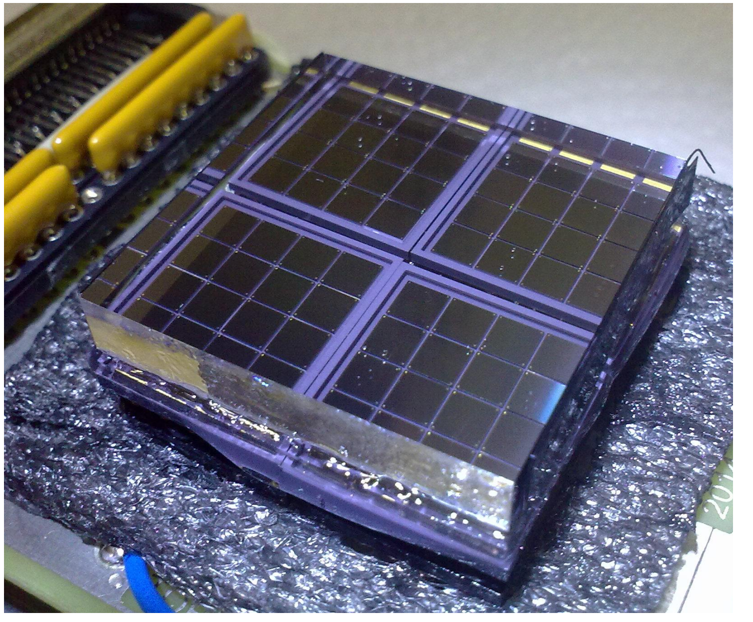

Prepare to commercialize the concept of self-calibrating clinical gamma camera

- build an operational prototype of self-calibrating clinical camera with upgraded front-end and acquisition electronics.
- achieve spatial and energy resolution, as well as acquisition rate comparable to those of commercial systems.
- characterize long term stability of the camera

Framework: Rad4Life